

Epithelial Fluid Transport: Protruding Macromolecules and Space Charges Can Bring about Electro-Osmotic Coupling at the Tight Junctions

A. Rubashkin^{1,2}, P. Iserovich², J.A. Hernández⁴, J. Fischbarg^{2,3}

¹Institute of Cytology, Russian Academy of Sciences, 194064 St. Petersburg, Russia

²Department of Ophthalmology, College of Physicians and Surgeons, Columbia University, W 168th St., New York, NY 10032, USA

³Department of Physiology and Cellular Biophysics, College of Physicians and Surgeons, Columbia University, 630 West 168th St., New York, NY 10032, USA

⁴Sección Biofísica, Facultad de Ciencias, Universidad de la República, Iguá esq. Mataojo, 11400 Montevideo, Uruguay

Received: 15 December 2005/Revised: 21 December 2005

Abstract. The purpose of the present work is to investigate whether the idea of epithelial fluid transport based on electro-osmotic coupling at the level of the leaky tight junction (TJ) can be further supported by a plausible theoretical model. We develop a model for fluid transport across epithelial layers based on electro-osmotic coupling at leaky tight junctions (TJ) possessing protruding macromolecules and fixed electrical charges. The model embodies systems of electro-hydrodynamic equations for the intercellular pathway, namely the Brinkman and the Poisson-Boltzmann differential equations applied to the TJ. We obtain analytical solutions for a system of these two equations, and are able to derive expressions for the fluid velocity profile and the electrostatic potential. We illustrate the model by employing geometrical parameters and experimental data from the corneal endothelium, for which we have previously reported evidence for a central role for electro-osmosis in translayer fluid transport. Our results suggest that electro-osmotic coupling at the TJ can account for fluid transport by the corneal endothelium. We conclude that electro-osmotic coupling at the tight junctions could represent one of the basic mechanisms driving fluid transport across some leaky epithelia, a process that remains unexplained.

Key words: Zeta potential — Charge selectivity — Epithelial cells — Helmholtz-Smoluchowski theory — Electro-osmosis — Leaky tight junction

Introduction

Fluid transport by epithelia is a fundamental process for which definitive understanding has eluded physiological research for many years. The idea that isotonic fluid transport across leaky epithelia is based on local osmotic phenomena has enjoyed favor among physiologists, as recently reviewed by Reuss (Reuss, 2000; 2006 (in press)). However, transcellular local osmosis is currently undergoing repeated questioning (Loo, Wright & Zeuthen, 2002; Sanchez et al., 2002; Shachar-Hill & Hill, 2002; Zeuthen, 2002; Hill Shachar-Hill & Shachar-Hill, 2004). For instance, in a recent model for an absorptive epithelium, isotonicity of the absorbate requires an important component of solute recirculation (Larsen, Sorensen & Sorensen, 2002). As another alternative we have reported evidence in favor of electro-osmotic coupling as the basis of corneal endothelial fluid transport (Sanchez et al., 2002). It is of course unclear whether all fluid transporting systems may achieve isotonic transport by similar means. In secretory glands, or in proximal kidney tubule, the geometry might allow local osmotic mechanisms to play roles. However, for flat leaky epithelia, given their relatively simpler geometry, arguments against local osmosis and in favor of alternative mechanisms appear stronger. In this framework, the purpose of the present work is to investigate whether the idea of epithelial fluid transport based on electro-osmotic coupling at the level of the leaky tight junction (TJ) (Sanchez et al., 2002) can be further supported by a plausible theoretical model.

Studies on electro-osmotic coupling in epithelia are scarce. In one of these studies the authors concluded that electro-osmotic coupling at the lateral intercellular space (LIS) was insufficient to account

for fluid reabsorption (McLaughlin & Mathias, 1985). On the other hand, the rapid development of fluid movements after application of electrical currents was taken as evidence for electro-osmosis across the paracellular pathway of isolated rabbit ileum by Naftalin and Tripathi (Naftalin & Tripathi, 1985). The possible role of tight junctions in coupling was stated in that study. That role was also touched upon in a review about the paracellular shunt of the proximal tubule in fluid transport (Weinstein & Windhager, 2001), in which the authors stated that: "A number of mathematical models of the proximal tubule, incorporating a permeable tight junction, were fashioned to try to reveal a role for the paracellular pathway in solute-solvent coupling, but these and subsequent models could not provide rationalization as to why electrical leakiness should correlate with the ability to transport isotonicity".

In the case of the corneal endothelium, we have recently argued that the LIS could not suffice for electro-osmotic coupling, and that the prime candidates for the site of such coupling were the leaky tight junctions (Sanchez et al. 2002). The finding that the mutagenic manipulation of charged residues in claudins 4 and 15 can create cation-or anion-selective channels in TJ (Colegio et al., 2002) is consistent with this possibility. A possible role of the tight junctions in water transport and in the regulation of Na^+ transport by the proximal tubule epithelium has also been discussed (Guo, Weinstein & Weinbaum, 2003; Weinstein 2003).

Background For The Model

Leaky tight junctions are characterized by the presence of rows of proteins in the gap between opposing cell membranes (Claude & Goodenough, 1973; Claude, 1978). These protein structures seem to be responsible for some of the junctional properties, such as the resistance to the passage of water and electrolytes and the charge selectivity (Colegio et al., 2003; Colegio et al. 2002). Therefore, this milieu cannot be described by a simplified model of electro-osmosis using the classical Helmholtz-Smoluchowski treatment, which was originally developed for the case of idealized capillaries with smooth surface (Tikhomolova & Kemp, 1993).

More realistic approaches for other geometries have already been developed in the fields of colloid chemistry and biophysics, such as those applied to electro phoresis and to the electro-kinetic behavior of red blood cells and liposomes (Donath, Pastushenko & Chizmadjev, 1978; Donath & Pastushenko, 1979; Jones 1979; Wunderlich 1982; Levine et al., 1983). For our case we combine two approaches, one to describe water flow and another to represent the electrical field. For the first one we utilize the Brinkman equation, a

hybrid between the Stokes and Darcy equations (Brinkman 1947), to describe the water flow across the TJ with its rows of protruding proteins. The Brinkman equation was originally developed to describe the hydrodynamics of water flow through polymeric layers, and has found its way into the modern physiological literature (Tada & Tarbell, 2000; Broday, 2002). For instance, it has been employed to analyze a hydrodynamic mechanosensory hypothesis for the brush border microvilli (Guo, Weinstein & Weinbaum, 2000). Secondly, we employ the Poisson-Boltzmann equation to represent the electrostatic field in the strand region of the TJ.

Some elements of our present approach can be found in prior treatments. For example, Donath & Voigt studied the electrostatic potential distribution in surfaces coated by a polyelectrolyte gel layer (Donath & Voigt, 1986b). These authors derived solutions for a system of hydrodynamic and electrostatic equations for the case of erythrocytes coated with long charged molecules. Other authors have investigated the influence of a gel layer coating on the electro-kinetic phenomena and streaming potentials in capillaries (Starov & Solomentsev, 1993; Starov, Bowen & Welfoot, 2001). In particular, these authors concluded that the Helmholtz-Smoluchowski equation becomes insufficient to describe that streaming potential at high values of porosity of the gel coat; they therefore modified that approach accordingly. Similarly, a description of electro-kinetic flow in a capillary with a charged surface layer has been obtained by solving the linearized Poisson-Boltzmann equation (Keh & Liu, 1995).

The strand area of the tight junction constitutes a distinct phase characterized by the presence of the fixed electrical charges carried by proteins such as claudin (Colegio et al., 2002, 2003). As a consequence, electrical potential differences will arise between this phase and free solution. Electrical potential differences in systems with fixed charges have been the subject of classical articles by Teorell, Meyer, and Sievers, as cited in a monograph (Lakshminarayanaiah, 1984). In addition, in order to understand the nature of the coupling process between the electrical current and the water flow at the leaky tight junction, it is of utmost importance to know the electrical conductivity at that level. As discussed below, it can be shown that in a macromolecular phase (TJ strand area), the dielectric constant of water will be lowered. Hence, in equilibrium, the energy of ion-medium interaction will be higher and the ionic concentration will be lower than in free solution (Vorotyntsev et al., 1993; Vorotyntsev, Rubashkin & Badiali, 1996; Bastug & Kuyucak, 2003). A general expression describing the electrostatic potential difference between microporous ion-exchange membranes and the electrolyte solution, and the influence of such potentials on electrokinetic

phenomena, has been developed (Romm & Rubashkin, 1983; Rubashkin, 1989). That expression will be employed here to analyze the potential drop between the TJ and the free solution. Finally, we shall utilize the Osterle method (Gross & Osterle, 1968) in order to represent the complete electrical field in the strand of the TJ as a sum of electromotive and quasi-equilibrium components (“electrostatic potential”). This method has been widely used in the analysis of electrokinetic phenomena (Sasidhar & Ruckenstein, 1981; Starov & Solomentsev, 1993). Some of the current findings indicating the theoretical possibility of electro-osmotic coupling in the tight junctions have been communicated in Abstract form (Fischbarg, Rubashkin & Iserovich, 2004).

Glossary

ABBREVIATIONS

HS Helmholtz - Smoluchowski
 EO electro-osmosis
 LIS lateral intercellular space
 TJ intercellular leaky tight junction
 Str strand regions in the leaky tight junctions

LATIN

c solute concentration in free solution
 c_{fix} concentration of fixed space negatively charged centers in the strand regions of the TJ
 $C_{\text{Na}}(x)$, $C_{\text{Cl}}(x)$ concentrations of Na^+ and Cl^- in the strand region of the TJ [Eq. 6]
 E_1 , E_2 electrical fields (along the z direction) in the LIS and the strand region of the TJ, respectively
 F Faraday’s constant
 h_1 , h_2 width of LIS and TJ
 I experimental value of the electrical current density across the entire epithelial layer
 I_1 , I_2 electrical current densities in LIS and in TJ ($I \times$ porosity)
 $I_{2(\text{Th})}$ theoretical electrical current densities in TJ [Eq. 15c]
 K_{per} permeability constant for TJ, [Eq. A2]
 k_{fr} friction coefficient between water and polymeric gel in TJ
 L_1 , L_2 lengths of LIS and TJ
 L_{B} Brinkman’s length for polymeric gel in TJ, [Eq. A2]
 L_{D} Debye screening length in free solution and in LIS [Eq. 12]
 $L_{2\text{D}}$ Debye length in TJ, [Eq. 12]
 L_{str} combined length of strand regions in the TJ (in the z direction)
 N_{A} Avogadro’s number
 n_1 , n_2 , n coefficient of distribution (or partition) for an ion between free solution and strand regions of the TJ [Eq. 6]

Q experimental value of the water flow density across the entire layer induced by a current density I .

Q_1 , Q_2 water flow densities in LIS and in TJ ($Q \times$ porosity)

Q_{IHS} water flow density in LIS by the HS equation [Eq. 1]

$Q_{2(\text{Th})}$ theoretical water flow density in TJ [Eq. 14a]

R_{g} gas constant

R total specific electrical resistance (LIS + TJ);

$R = R_1 + R_{\text{str}} + R_2$

R_1 specific electrical resistance of LIS = $L_1/(\kappa S_1)$

R_{str} , R_2 specific electrical resistance in the TJ; strand region: $R_{\text{str}} = L_{\text{str}}/(\kappa_2 S_{\text{str}})$; non-strand region:

$R_2 = (L_2 - L_{\text{str}})/(\kappa S_2)$

R_{TJ} total specific electrical resistance of the TJ ($R_{\text{TJ}} = R_{\text{str}} + R_2$)

r , $r_{2(\text{Th})}$ coupling coefficients between current and fluid movements (experiment and theoretical) [Eqs. 2a, 14b, 16]

S_1 average cross section of the LIS (for 1 cm^2 of the cell layer)

S_2 cross section of the TJ (for 1 cm^2 of the cell layer)

S_{str} cross-section of the strand region of the TJ

T absolute temperature

Th, exp suffixes indicating theoretical and experimental values

t_{Na} , t_{Cl} transference numbers for Na^+ and Cl^- in free solution

U_{Na} , U_{Cl} ion mobilities

$v_2(x)$ velocity of water in TJ

ΔV potential difference (electromotive force)

ΔV_1 potential difference along the LIS

ΔV_2 potential difference across the strand region of the TJ

w_1 , w_{str} porosity ($1/S_1$; $w_1 S_1/S_{\text{str}}$) of the LIS, and of the strand region of the TJ of the corneal endothelial layer

x , z coordinates normal, parallel to the direction of water flow in the TJ

$y(x)$ [$\phi(x) - \phi_D$], difference between electrostatic and phase potentials in the TJ strand region; [Eqs. 10a, 11, 13a, 13b]

z_{fix} charge number for TJ strands

GREEK

β ratio between concentrations of fixed space charges in the strand region of the TJ, and the bulk medium ($\beta = c_{\text{fix}}/c$)

ε water dielectric constant at 35°C

ε_0 permittivity of free space

η viscosity of water

κ conductivity in free solution of NaCl at $c = 0.15$ mol/L

κ_2 conductivity in the TJ strand; Eq. 15a

ζ_1 membrane zeta potential in the surface of the LIS

ζ_2 membrane zeta potential in the surface of the TJ

$\rho_2(x)$ space charge density in TJ; [Eq. 11]

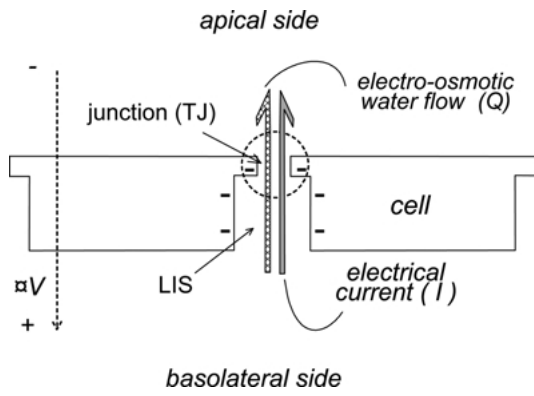


Fig. 1. Diagram of a leaky epithelial cell layer, showing the tight junctions as the site for electro-osmotic coupling. An electrical current (I) and fluid movement (Q) traverse the paracellular pathway. The epithelium transports fluid and electrolytes as a secretory layer (in the “backwards” direction).

$\rho_{\text{mov}}(x)$ space charge densities of the movable charges; [Eqs. 7, 13b]

$\rho_{\text{fix}} [F z_{\text{fix}} c_{\text{fix}}]$, space charge density of macromolecules in strand regions of TJ

$P_{\text{fix}}[\rho_{\text{fix}}/(F c)]$, dimensionless fixed charge density in the volume of the TJ strand regions

σ_2 surface charge density in the TJ membrane; [Eq. 3a]

$\delta_2 \delta_2 = h_2/2$, half-width of TJ

ϕ_D phase potential, Eq. 10b

$\psi(x,z)$ total electrical potential

$\phi(x,z)$ equilibrium component of the electrical potential (electrostatic potential)

$\psi(z)$ non-equilibrium component of the electrical potential

$\mu_{\text{Na}}^{(0)}, \mu_{\text{Cl}}^{(0)}$ standard chemical potentials of ions in free solution (ion-solution energy of interaction)

$\mu_{\text{Na}}^{(\text{TJ})}, \mu_{\text{Cl}}^{(\text{TJ})}$ standard chemical potentials of ions in strand regions of TJ (ion-solution energy of interaction)

$\Delta\mu_{\text{Na}}^{(0)}, \Delta\mu_{\text{Cl}}^{(0)}$ difference in standard chemical potential in free solution

Results and Discussion

THEORY

We consider a model epithelial layer, such as the one pictured schematically in Fig. 1. We assume that the concentrations of the solutions at the apical and basolateral compartments in this model are equal. This implies that small local gradients that cellular transport of electrolytes may generate in the immediate vicinity of line cell are neglected. (Sanchez et al., 2002). We assume that the only asymmetry arises from the polarized distribution of electrogenic transporters and channels on both sides of the cell. This results in an electrical potential difference across

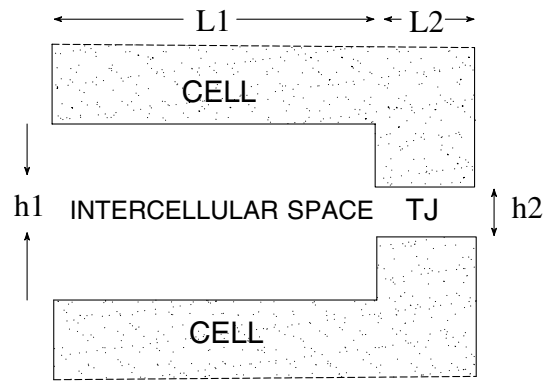


Fig. 2. Schematic diagram of a region with two adjoining corneal endothelial cells, highlighting the intercellular space and the leaky tight junction separating them. The basal (stromal) side is at the left, apical (aqueous) to the right. Symbols denoting dimensions are explained in the glossary and the text.

the epithelial layer (for corneal endothelium: Fischbarg, 1972; Barfort & Maurice, 1974; Hodson, 1974), which is the driving force for water transport in this context.

BASIC ASSUMPTIONS AND GENERAL ASPECTS OF THE ANALYSIS

In what follows, we shall advance theoretical arguments to support the idea that the corneal endothelial leaky tight junctions represent the sites at which electrical flow generates water flow across that cell layer. For that purpose, we shall refer to the scheme depicted in Fig. 1 for a leaky epithelium in general. As shown in Figs. 1 and 2, the paracellular pathway consists of two channels in series, the lateral intercellular space (LIS) and the leaky tight junction (TJ). We shall analyze them separately.

STANDARD CURRENT AND WATER FLOW FOR THIS ANALYSIS

Throughout this treatment we compare theoretical results with those obtained from the experimental application of electrical current across in vitro rabbit corneal endothelium. We assume the application of the experimental current density in all cases, $I = 10.5 \mu\text{A cm}^{-2}$, which, as we have demonstrated (Sanchez et al., 2002; Fig. 3 in that paper), will induce a fluid flow of $Q = 2.48 \mu\text{L hr}^{-1} \text{cm}^{-2} = 6.9 \text{ nm s}^{-1}$.

THE CONTRIBUTION OF ELECTRO-OSMOSIS IN THE LATERAL INTRACELLULAR SPACE (LIS)

In contrast to the TJ strand region, the LIS is relatively wide and devoid of protruding proteins in significant amounts. Hence, the classical Helmholtz-Smoluchowski (HS) approach can be used here (Kruyt 1952; Hanter, 1981; Tikhomolova & Kemp,

1993). For the LIS, the HS water flow density Q_1 would be:

$$Q_1 = -\frac{\varepsilon\varepsilon_0 E_1 \zeta_1}{\eta} \quad (1)$$

We shall utilize Eq. 1 to obtain a value for Q_1 (*see* Glossary for the meaning of the rest of the symbols) and to compare it with an experimental one. For corneal endothelium, from our published experimental date (Sanchez et al., 2002), the coupling coefficient r between fluid and current movement is:

$$r = \frac{Q}{I} = 2.37 \times 10^8 \frac{\mu\text{m}^3}{\text{hr}\mu\text{A}} \quad (2a)$$

Due to the smaller across section, water flow in the LIS is faster than in the bulk (*see* Fig. 1). From the tissue geometry, the width of LIS is: $h_1 \approx 30$ nm, and, given the total perimeter of cells and the width of the LIS, the relevant factor or “porosity” w of the rabbit corneal endothelial layer is $w = 92$. As always in this context, we assume the application of a steady current of $I = 10.5 \mu\text{A cm}^{-2}$ across the corneal endothelium, resulting in a bulk translayer water flow of value Q above. Hence, the water velocity Q_1 in the LIS will be:

$$Q_1 = w \times Q = 0.63 \mu\text{ms}^{-1}$$

To compute the value of the electrical potential difference ΔV_1 along the LIS required for Eq. 1 above, we resort to Ohm’s law:

$$\Delta V_1 = -\frac{w I L_1}{\kappa} = -0.055 \text{ mV}; \quad (2b)$$

In Eq. 2, $\kappa = 21.1 \cdot 10^{-3} \text{ S cm}^{-1}$ is the conductivity of a NaCl solution calculated at $c = 0.15 \text{ mol/L}$ and 35°C (Harned & Owen, 1958, p. 234). $L_1 = 12 \mu\text{m}$ is the length of the LIS. In this context, the electrical current density in the LIS is $I_1 = I \cdot w = 962 \mu\text{A cm}^{-2}$, and the electrical field along the LIS will be: $E_1 = -\Delta V_1/L_1 = 4.56 \text{ V/m}$, both relatively moderate values. As for ζ_1 , from the literature, the zeta potential (ζ) of typical cell membranes is approximately -15 mV (McLaughlin & Mathias, 1985), (although smaller values have been reported, i.e., -9 mV (Pasquale et al., 1990)). Using a value of $\zeta_1 = -15 \text{ mV}$, plus values of: viscosity $\eta = 6.9 \cdot 10^{-3}$ poise, $\varepsilon = 78.5$ and $\varepsilon_0 = 8.85 \text{ pF m}^{-1}$, from the HS equation (Eq. (1) the theoretical EO water flow (Q_{IHS}) in the LIS is: $Q_{\text{IHS}} = 0.07 \mu\text{m s}^{-1}$, about 10 times smaller than the experimental value.

Hence, as mentioned above, Helmholtz-type electro-osmosis in the LIS cannot generate the experimental transendothelial water flow typically determined (e.g., Sanchez et al., 2002). For electro-osmosis to be possible, coupling would have to take place at the junctions. For this reason, we turn to an analysis of the water flow in leaky tight junctions.

ELECTRO-HYDRODYNAMIC MODEL OF THE LEAKY TIGHT JUNCTION (TJ)

Figures 2 and 3 present schematically a model for the TJ. As mentioned in the Introduction, the cell membranes limiting the TJs possess surface electrical charges. According to the Gouy-Chapman theory (Kruyt, 1952; Hanter, 1981), the value of this charge is given by:

$$\sigma_2 = \sqrt{8\varepsilon\varepsilon_0 R_g T} \sqrt{c} \sinh \left(\frac{F\zeta_2}{2R_g T} \right). \quad (3a)$$

As mentioned above, the zeta potential of cell membranes including those limiting the TJs is presumably between -9 and -15 mV . Taking $\zeta_2 = -10 \text{ mV}$, it follows that $F\zeta_2/(2R_g T) \approx 0.187$, and we can approximate the hyperbolic sine expression above. Therefore, we write Eq. (3a) as:

$$\zeta_2 \approx \frac{L_D}{\varepsilon\varepsilon_0} \sigma_2; \quad (3b)$$

Importantly, for the strand region of the TJ a volume electrical charge must also be considered in addition to the surface charge (*see* Fig. 3). As mentioned above, there is evidence (Colegio et al., 2003; Colegio et al., 2002) that charges in claudins can be correlated with charge-selectivity in the TJ. How the charges are distributed spatially is not known in detail at this time, as there are no known 3-D structures for TJ proteins. Still, there is a TJ model (Van Itallie & Anderson, 2004) in which claudin extracellular loops protrude into the junction forming pores surrounded by charged residues (cf. also Fig. 3B here).

We will therefore assume that the spatially fixed-charge centers will be found where the rows of proteins (strands) appear in the junction. In our arrangement, there are fixed charges at uniform volume and surface concentrations (c_{fix} and σ_2 , respectively) in the volume and membranes of the strand regions of the TJ. In the rest of the volume in the junction, in between the protein strands, the concentration of fixed charges in the volume is presumed to be much less, while there will be surface charges σ_2 in the cell membranes.

In order to determine the water flow across the TJ, it is necessary to know the density of movable charges in that medium. The value of such density will differ from the one in the LIS or free solution as a consequence of the existence of a complex charged macromolecular arrangement in the strand regions of the TJ aqueous path. In addition, this fact also determines the existence of important frictional interactions between the ions and the macromolecules in the TJ. For this reason the HS expression cannot be used, and other expressions for the water flow and

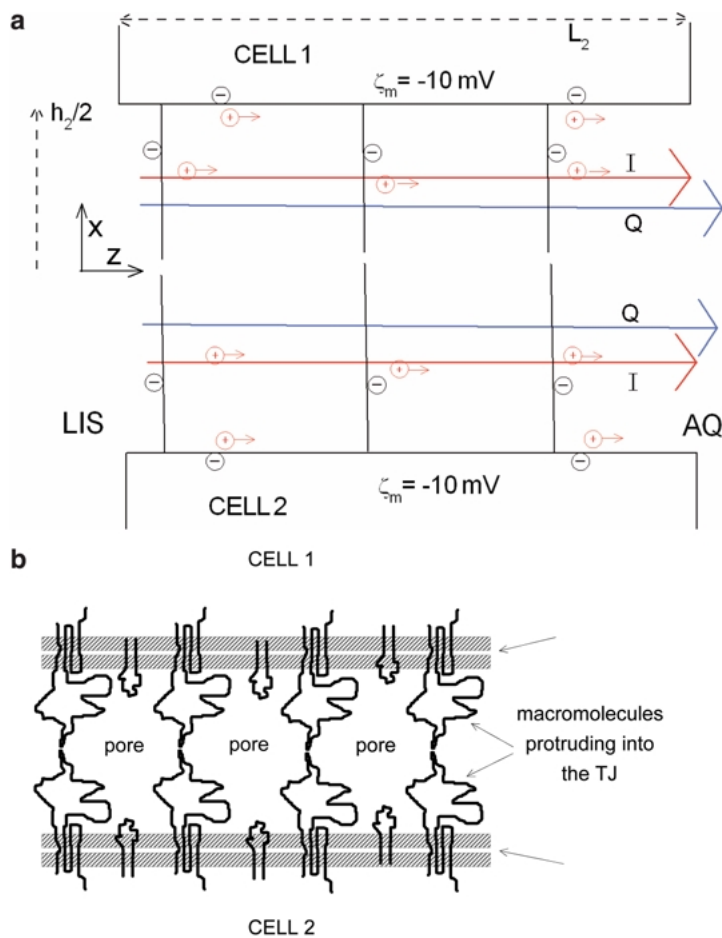


Fig. 3. Schematic diagram of the leaky tight junction. Junctional width is $h_2 \sim 45 \text{ \AA}$, and junctional length is $L_2 \sim 1 \text{ \mu m}$. (A) Three rows of charged structures (e.g., claudins) bearing negative charge are shown as thin protrusions. The combined length of strand regions is $L_{str} \sim 0.1 \text{ \mu m}$ (not shown; for the possible 3-D appearance of these protrusions, see Van Itallie & Anderson, 2004). There are also structural elements protruding into the junction (e.g., cadherins, occludins; not shown). The diagram also shows the fixed negative charges lining the walls of the junction, which are accounted in our treatment as the zeta potential ζ_m . For simplicity, only positive movable charges are shown (circles with arrows). Movements of positive charge (I) and resulting electrical osmotic fluid movement (Q) are also depicted (B). Side view at the plane of one of the strands above.

the electrical current traversing the TJ need to be derived.

We model the membranes limiting the TJ as parallel plates (see Fig. 3), with the x axis perpendicular to the membrane surface and $x = 0$ located at the center of the tight junction. We assume that, as in other leaky epithelia (Claude & Goodenough, 1973; Claude 1978), the endothelial TJs have roughly parallel strands or rows of macromolecules limiting passage of water and solutes across it. Leaky epithelial TJs tend to have only a few rows (fences) of strands; we assume that there are three rows present in our case (Fig. 3). For the width of the TJ we choose a value of 45 \AA . From hydraulic flows across corneal endothelium, the TJ would be equivalent to an idealized slit 39 \AA wide and 1 \mu m long (Fischbarg, Warshavsky & Lim, 1977). In addition, these TJs are permeable to horseradish peroxidase (Kaye, Sibley & Hoefle, 1973), for which we estimate a diameter of 45 \AA . We have therefore assumed for the TJ a width h_2 of 45 \AA , while the restrictions in the strand regions would decrease that width by 20%.

The characteristics of the strand region essentially determine the electrical resistance of the entire TJ. The specific resistance of both freshly excised and

cultured corneal endothelial layers is about 25 ohm cm^2 . Recent data (Kuang et al., 2004) indicate that, of such total, the TJ contribute ~ 20 and the LIS $\sim 5 \text{ ohm cm}^2$.

ELECTRICAL FIELD ACROSS THE STRAND REGION

In developing the model, we need to set a value for the combined length of the strand region in the TJ (L_{str}). With the other parameter values chosen, correspondence between theory and experimental results (cf. Figs. 4 and 5) is achieved if $L_{str} = 100 \text{ nm}$, or 10% of the total TJ length L_2 . If the strand regions are formed only by the three strands exemplified in Fig. 3, assuming that the proteins involved are $\sim 30 \text{ \AA}$ wide, juxtaposition of all three would yield only $\sim 10 \text{ nm}$ instead. This difference may mean that additional macromolecules may be protruding into the TJ, or that yet unspecified characteristics of the TJ somehow optimize its behavior towards electro-osmotic coupling. Given the value of 100 nm set for L_{str} , the electrical field across each of the strand regions will be very large ($\sim 1 \text{ kV/m}$), and will be determinant in the generation of electro-osmotic coupling.

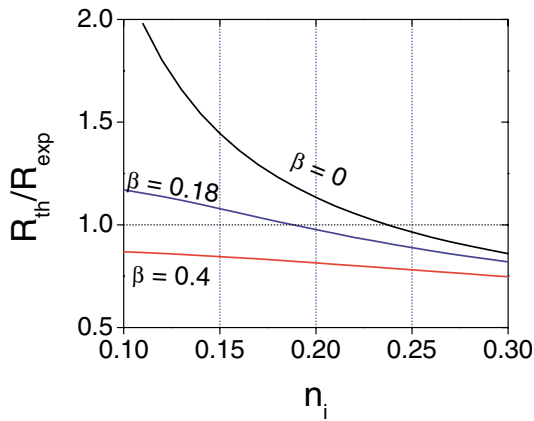


Fig. 4. Specific electrical resistance across the endothelial layer as a function of the partition coefficient n_i for ions inside the strand region of the TJ. Curves are computed for of three different values assumed for the normalized fixed charge ($\beta = c_{\text{fix}}/c$). The computed resistance was normalized using that from experimental determinations (Sanchez et al. 2002), as detailed in the text. The graph is useful to delimit a set of parameter values for which there is a resistance ratio of 1, signifying agreement between theory and experiment.

There will also be segments of the TJs in between strands (Fig. 3). The fixed charges present in the TJ membranes in there would add an electro-osmotic component upon the passage of current. However, the field would be relatively small, like that in the calculation of HS electro-osmosis in the LIS [Eq. 1]. Calculations show that such a component would be of the order of 5% of the water flow through the TJs; we have therefore chosen to neglect it.

THE MODIFIED BRINKMAN EQUATION

The Reynolds number for the water transport across epithelial layers is generally very small (McLaughlin & Mathias, 1985) (as are the water velocities), hence the inertial terms of the Navier-Stokes equation are negligible by comparison with the viscous terms. For this reason, instead of the Navier-Stokes equation, we need to utilize an alternative version of the Stokes equation (Happel & Brenner, 1983). For the water flow across the strand region of the TJ we employ the Brinkman equation (Brinkman, 1947), an expression originally developed to describe flow across polymeric media. As mentioned, the Brinkman equation is a hybrid between the Stokes and Darcy equations. It considers the following basic aspects: a) the existence of friction between water and the macromolecular media; and b) the existence of a water velocity profile $v(x)$ normal to the membranous wall. In our case, the Brinkman differential equation for the fluid flow velocity v_2 in the strands of the TJ reads (*see Glossary for the meaning of the symbols*):

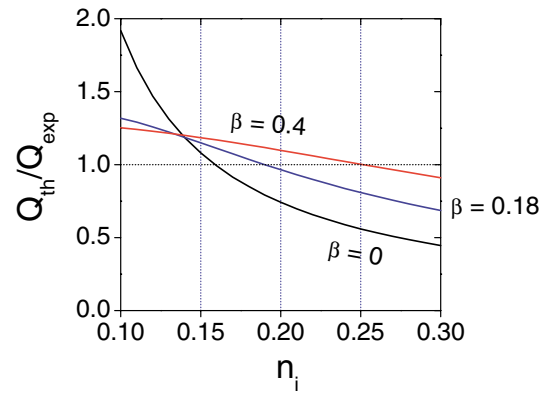


Fig. 5. Water flow across the endothelial layer as a function of the partition coefficient n_i for ions inside the strand region of the TJ. Curves are computed for of three different values assumed for the normalized fixed space charge ($\beta = c_{\text{fix}}/c$). The computed water flow was normalized using that from experimental determinations (Sanchez et al., 2002), as detailed in the text. The graph is useful to delimit a set of parameter values for which there is a resistance ratio of 1, signifying agreement between theory and experiment

$$\eta \frac{d^2 v_2}{dx^2} + E_2 \rho_{\text{mov}}(x) - k_{fr} v_2(x) = 0 \quad (4a)$$

with boundary conditions ($\delta_2 = h_2/2$):

$$v_2(-\delta_2) = v_2(\delta_2) = 0 \quad (4b)$$

The second term in Eq. 4a represents the force exerted by the movable electrical charge on the water; this term is absent the original Brinkman equation. If the third term is also absent Eq. 4a becomes the classical Stokes equation. As can be seen, the electrical force term of Eq. 4a is given by the product between the TJ electrical field and the volume density of the movable charges. Therefore, we need to derive expressions to evaluate their values. As we do this below, according to the Osterle method (Gross & Osterle, 1968), the electrical potential Ψ will be understood to include two parts, equilibrium ϕ depending on the fixed charges, and non-equilibrium ψ , the translayer potential difference giving rise to the electrical current I :

$$\Psi(x, z) = \psi(x, z) + \phi(x, z)$$

In the case of Eq. 4a the field is generated by the non-equilibrium electrical potential:

$$E_2 = - \frac{d\psi(z)}{dz}$$

PARTITION OF IONS IN THE TJ

A first step towards describing quantitatively the physical chemistry of the fluid in the TJ regions is to examine its ionic population. Due to the presence of

macromolecules in this phase, we consider it to be different from the “free solution” phase. Hence, the standard chemical potential of an ion in the TJ medium will be different from that in free solution. This phenomenon can be understood by utilizing the Born expression given in Eq. 5a below (as in Bastug & Kuyucak, 2003) to calculate the interaction energy between an ion and its medium. This energy is the sum of all the interactions potentials, which include van der Waals and image potentials. Hence, the standard chemical potential of from in the TJ will differ from that in free solution. In mathematical terms for Na^+ one has:

$$\mu_{\text{Na}}^{\text{TJ}} - \mu_{\text{Na}}^{(0)} = \frac{N_A e^2}{2\epsilon_0 \Gamma_{\text{Na}}} \left[\frac{1}{\epsilon_{\text{TJ}}} - \frac{1}{\epsilon} \right] \quad (5a)$$

where r_{Na} is the crystal radius of Na^+ , ϵ is the dielectric constant for water in free solution, and ϵ_{TJ} is the dielectric constant for the TJ strand medium.

At equilibrium, equations for the relations between the electrochemical potentials of the sodium and chloride ion in free solution and inside the TJs can be written as:

$$\begin{aligned} \mu_{\text{Na}}^{(0)} + R_g T \ln(c) &= \mu_{\text{Na}}^{(\text{TJ})} \\ &+ R_g T \ln(C_{\text{Na}}(x)) + F\varphi_2(x) \\ \mu_{\text{Cl}}^{(0)} + R_g T \ln(c) &= \mu_{\text{Cl}}^{(\text{TJ})} \\ &+ R_g T \ln(C_{\text{Cl}}(x)) + F\varphi_2(x) \end{aligned} \quad (5b)$$

In Eq. 5b, $\mu^{(0)}$ and $\mu^{(\text{TJ})}$ represent the standard chemical potentials of the corresponding ions in free solution (0) and in the strand regions of the TJ, respectively; c is the NaCl concentration in free solution. The $C(x)$'s are the corresponding concentrations at point “ x ” of the TJ, and $\Phi_2(x)$ is the electrostatic potential at the same position. We consider the electrostatic potential of the free solution to be zero. To be noted, $\Phi_2(x)$ represents the equilibrium part of the electrical potential in Eq. 4c.

From Eq. 5b, the concentration of each ion in the strand regions of the TJ will be given by

$$\begin{aligned} C_{\text{Na}}(x) &= cn_1 \exp(-F\varphi_2(x)/R_g T); \\ n_1 &= \exp\left(\left(\mu_{\text{Na}}^{(0)} - \mu_{\text{Na}}^{(\text{TJ})}\right)/R_g T\right) \\ C_{\text{Cl}}(x) &= cn_2 \exp(-F\varphi_2(x)/R_g T); \\ n_2 &= \exp\left(\left(\mu_{\text{Cl}}^{(0)} - \mu_{\text{Cl}}^{(\text{TJ})}\right)/R_g T\right) \end{aligned} \quad (6)$$

Here, n_1 and n_2 are partition coefficients. With the aid of Eqs. 6 we can obtain the following expression for

the volume density of movable charges in the medium of the strand region of the TJ:

$$\begin{aligned} \rho_{\text{mov}}(x) &= Fc \left(\exp\left[\frac{-\Delta\mu_{\text{Na}}^{(0)} - F\varphi_2(x)}{R_g T}\right] \right. \\ &\quad \left. - \exp\left[\frac{-\Delta\mu_{\text{Cl}}^{(0)} + F\varphi_2(x)}{R_g T}\right] \right) \end{aligned} \quad (7)$$

To be noted, in Eq. 7 the μ 's can be interpreted in terms of the difference in the energies of interaction between ions and medium in LIS and the TJ strand regions. Such interaction energies have been employed previously (Starov et al., 2001; Starov & Solomentsev, 1993) in order to analyze electrokinetic phenomena. This can be used to simplify Eq. 7. To this end, we assume here that, both for the sodium and chloride ions, the terms $\exp(-\Delta\mu^{(0)})$ of Eq. 7 approximately equal the partition or distribution coefficient n (we assume, for simplicity, that $n_1 = n_2 = n$ see Glossary). Under this assumption substitution of the movable charge from Eq. 7 into the Poisson equation yields an equation for the electrostatic potential in the strand region of the TJ:

$$\begin{aligned} \frac{d^2\varphi_2}{dx^2} &= -\frac{1}{\epsilon\epsilon_0} [Fcn(\exp(-F\varphi_2(x)/R_g T) \\ &\quad - \exp(F\varphi_2(x)/R_g T)) + \rho_{\text{fix}}] \end{aligned} \quad (8)$$

The boundary conditions are given by the application of the Gauss condition at the membrane of the TJ strand regions:

$$\left. \frac{d\varphi_2}{dx} \right|_{(-\delta)} = -\frac{\sigma_2}{\epsilon\epsilon_0}; \quad \left. \frac{d\varphi_2}{dx} \right|_{(\delta)} = \frac{\sigma_2}{\epsilon\epsilon_0} \quad (9)$$

Since the surface charge density is comparatively small, we can linearize equation 8. For this, we introduce a new variable $y(x)$ defined as:

$$y(x) = \varphi_2(x) - \varphi_D \quad (10a)$$

Here, $y(x)$ is the difference between the electrostatic potential at x and a newly defined Φ_D phase potential between the free solution and the strand region of the TJ. This phase potential Φ_D is given by:

$$\varphi_D = -\frac{RT}{F} \ln\left(-\frac{Z_{\text{fix}}c_{\text{fix}}}{2nc} + \sqrt{\left(\frac{Z_{\text{fix}}c_{\text{fix}}}{2nc}\right)^2 + 1}\right) \quad (10b)$$

As mentioned above, the membrane surface charge is small. Hence, the electrical potential difference $y(x)$

Eq. 10a is also sufficiently small [i.e., $(Fy(x)/R_gT) \ll 1$]. This allows us to obtain the desired linear approximation for the total volume charge density (movable plus fixed, to go into Poisson's equation) for the strand region of the TJ (Eq. 7):

$$\rho_2(x) = F \left[c_n \exp\left(-\frac{F\varphi_2(x)}{R_gT}\right) - c_n \exp\left(\frac{F\varphi_2(x)}{R_gT}\right) + z_{fix}c_{fix} \right] \cong -\frac{y(x)}{(L_{D2})^2} (\varepsilon\varepsilon_0) \quad (11)$$

In this expression L_{D2} is the Debye length in the strand regions of the TJ. It depends on the phase potential and on the Debye length L_D in free solution (*see* Glossary) as follows:

$$L_D = \sqrt{\frac{\varepsilon\varepsilon_0 R_g T}{2cF}}; L_{D2} = \frac{L_D}{\sqrt{n} \sqrt{\cosh(F\varphi_D/R_gT)}} \quad (12)$$

From Eqs. 12, the Debye length in free solution is $\sim 8 \text{ \AA}$ ($c = 0.15 \text{ mole/L}$), but in the TJ strand regions it will be larger. At relatively small parameter n values, if the fixed charges are present only in the membranes, the electrostatic potential from one membrane will influence the opposite membrane, and there will be overlap between the diffuse segments of the double layers. As a result, the concentration of counterions will exceed that of co-ions, and the TJ will exhibit large selectivity.

From Eqs. 3b, 8, and 11, we can obtain the following expression for the distribution of the electrostatic potential in the TJ:

$$y(x) = \left(\frac{\zeta_m}{\sqrt{n} \cosh(F\varphi_D/R_gT)} \right) \frac{\cosh(x/L_{D2})}{\sinh(\delta_2/L_{D2})}; \varphi_2(x) = \varphi_D + y(x) \quad (13a)$$

From Eq. 11, the density of movable charges in the strand regions of the TJ is given by

$$\rho_{mov}(x) = F[C_{Na}(x) - C_{Cl}(x)] \cong -z_{fix} Fc_{fix} - (\varepsilon\varepsilon_0) \frac{y(x)}{(L_{D2})^2} \quad (13b)$$

WATER FLOW AND COUPLING COEFFICIENT

Using the movable charge density obtained in Eq. 13b, the Brinkman equation Eq. 4 can be solved to yield Eq. A3a for the water velocity profile in the TJ. A detailed treatment is shown in Appendix A. In summary, integration of Eq. A3a across the width of the TJ yields the following expression (cf. Eq. A4c) for the theoretical water flow across the TJ:

$$Q_2 = -\frac{Fc_{fix}E_2}{\eta} (L_B)^2 f - \frac{\varepsilon\varepsilon_0 E_2 \zeta_2}{\eta} p \quad (14a)$$

The value of $Q_2(\text{Th})$ is used in the expression $Q_2(\text{Th})/Q_2(\text{exp})$ to generate the data shown in Fig. 5. It is also useful to calculate the theoretical coupling ratio for the junction:

$$r_2(\text{Th}) = \frac{Q_2(\text{Th})}{I_2(\text{Th})} \quad (14b)$$

To be noted, for the Brinkman length in Eqs. 14a and 16 we take: $L_B = 45 \text{ \AA}$, since this parameter (*see* Appendix A) characterizes the friction of water with the TJ and should be of the order of the width of the TJ, set at 45 \AA . In Eq. 14a, f (defined in Eq. A4b) is a function of the width of the TJ and of the Brinkman length L_B (defined in Eq. A2), while p depends on the Debye length in the TJ, the width of the TJ, and the Brinkman length (*see* Glossary and Eqs. A4a - A4b). The first term in Eq. 14a represents the influence of the volume charge on the generation of volume flow by the electrical field in the TJ. The second term is similar to the Smoluchowski equation with one important difference: the parameter p takes into account the friction between water flow and the macromolecules in the volume of the tight junction. In addition, from Eqs. 12 and A4b, p goes approximately like $1/n$; this will explain some of the results below.

ELECTRICAL CONDUCTIVITY IN THE TJ

We will now evaluate the electrical conductivity κ_2 of the strand regions of the TJ and the electrical current density across it. An expression for it can be obtained by integrating the ionic concentration profiles along the cross section of the TJ (*see* Appendix B):

$$\kappa_2 = F^2 n b c \left[U_{Na} e^{-F\varphi_D/R_gT} \left(1 - \alpha \frac{F\zeta_2}{R_gT} \right) + U_{Cl} e^{F\varphi_D/R_gT} \left(1 + \alpha \frac{F\zeta_2}{R_gT} \right) \right] \quad (15a)$$

In Eq. 15a, the factor b represents the fraction by which the ionic mobility in the TJ strand region is less than that in free solution. In Appendix B we give an estimate, from which $b \approx 0.45$. This allows one to find the specific electrical resistance of the TJ strand region as

$$R_{str} = L_{str}/(\kappa_2 S_{str}) \quad (15b)$$

As shown in Appendix B, using this expression one can go on to compute the total theoretical resistance $[R_{TJ}(\text{Th})]$ of the TJ. The ratio $R_{RJ}(\text{Th})/R_{TJ}(\text{exp})$ is what is plotted in Fig. 4 is a function of the partition coefficient for ions inside the TJ.

Using Eq. (15a), we can find the electrical current I_2 in the TJ. One has simply:

$$I_2 = E_2 \kappa_2 \quad (15c)$$

Substituting, into Eq. 14b, we will obtain the theoretical coupling ratio:

$$r_2(\text{Th}) = -\frac{F c_{\text{fix}}}{\eta \kappa_2} (L_B)^2 f - \frac{\varepsilon \varepsilon_0 \zeta_2}{\eta \kappa_2} p \quad (16)$$

Equations 14–16 constitute the main results of this paper.

Discussion of the Results

The theoretical results are seen to depend on three main parameters: the coefficient for ionic distribution (“partition coefficient”) n , the surface charge density at the TJ membrane as reflected in the membrane zeta potential ζ_2 and the dimensionless concentration of fixed charges of the bulk of the TJ, $\beta = c_{\text{fix}}/c$. We consider the effects of these parameters on the specific resistance of the TJ, and on the water flow.

As mentioned above, we used Eqs. 15a–15b to calculate electrical conductivity and electrical resistance of the TJ, and Eq. 14a to calculate water flow. The results plotted in Figs. 4 and 5 are dimensionless, as in both cases, the values calculated theoretically were divided by the experimental values. To estimate the experimental value of R_{TJ} , we start from a reported value of 28.5 ± 0.6 ohm cm^2 for the total specific resistance of rabbit corneal endothelial cells cultured for two weeks (Kuang et al., 2004). We then compute the specific resistance of the LIS ($R_1 = L_1/(\kappa S_1 = 5.2$ ohm $\text{cm}^2)$), and we obtain as the difference an estimate of $R_{\text{TJ}} = 22.6$ ohm cm^2 . For the junctional flow density (or flow velocity), we calculate $Q_2 = Q \times w_{\text{str}} = 18.8$ $\mu\text{m s}^{-1}$.

Figs. 4 and 5 show these results. In Fig. 4, as the partition coefficient increases, the ionic concentration in the TJ would be expected to increase, causing a decrease in R_{th} and hence in the ratio $R_{\text{th}}/R_{\text{exp}}$. All three curves show such, decrease. As for the dependence of $R_{\text{th}}/R_{\text{exp}}$ on fixed space charge concentration, as that charge increases, the counterion concentration would be expected to increase, producing again a decrease in R_{th} and hence in the ratio $R_{\text{th}}/R_{\text{exp}}$. Once more, the data conform to the expectation.

In Fig. 5, events are somewhat more complex. As the partition coefficient increases, again the ionic concentration in the TJ and hence the junctional conductance would be expected to increase. However, in all cases, this results in a decrease of the theoretical water flow (and of $Q_{\text{th}}/Q_{\text{exp}}$). A reason for this can be gleaned from Eq. 16 for the theoretical coupling ratio (water flow per unit current). In it, the junctional conductance κ_2 is in the denominator (as well as the

viscosity). Intuitively, conductance acts like viscosity: the more of it the less efficient the system is at generating water flow. As for space charges, there is a cross-over at $n = 0.13$. For larger n values, increasing space charges increase $Q_{\text{th}}/Q_{\text{exp}}$. This improvement in water flow may be expected intuitively if increased space charges would recruit additional movable counterions to communicate the momentum of their water shells to the fluid.

As can be seen, in Fig. 4 the predicted resistance decreases with space charge, while in Fig. 5 the predicted fluid flow increases with space charge. In both cases, increasing the partition coefficient leads to a worsening of the predictions. In spite of these complexities, there is a region for which theory and experiment agree for both R and Q . For the middle curve in both figures, the value of the relative fixed space charge β was set at 0.16 to emphasize this point; in both cases, agreement is obtained with a value for the partition coefficient of $n \approx 0.19$.

The picture that emerges therefore shows the strand region of the TJ to be a place that ions populate only with great difficulty, since the partition coefficient n is relatively low compared with free solution. The conductance in that region (calculated with Eq. 15) is also relatively low, which is consistent with the above; one has $\kappa_2 = 0.13 \kappa$ (see Appendix B for further details).

Lastly, the EO process that occurs at the TJ cannot be considered to correspond to a Schmid-type of electro-osmosis (Schmid, 1950; Schmid & Schwarz, 1952). Such approach would not introduce the above-mentioned modifications in the standard chemical potentials, an effect that we consider to play a relevant role in the process of electro-osmotic coupling at the leaky tight junction. Besides, the occurrence of a Schmid-type of electro-osmosis at the level of the leaky tight junction would require very large concentrations of fixed electrical charges, of the order of the concentration of electrical charges in free solution. As mentioned above, the results in Figs. 4 and 5 suggest otherwise, as best agreement is found for a β value of ≈ 0.19 . In addition, recent evidence also tends to militate against this, as changes in the sign of a single claudin residue can significantly modify the cation-anion selectivity of the TJ (Colegio et al., 2002). One would expect such change to be drowned out if β would be relatively large.

Summary and Conclusions

The mere fact that in spite of the difficulties of this analysis it is possible to find a constellation of parameters for which theory agrees with experiment appears quite significant. The analysis performed in this study allowed us to develop a novel formal basis to describe electro-osmotic water flow across the tight

junctions of leaky epithelia. The application of this theoretical analysis to the case of the corneal endothelium supports our prior conclusion that isosmotic water flow across this tissue fundamentally occurs via electro-osmotic coupling across the leaky tight junctions. The water flow is therefore ultimately the consequence of the physiological maintenance of an electric potential difference across the overall tissue.

From this analysis, efficient electro-osmotic coupling would occur due to unique environmental characteristics to be found only in the strand regions of leaky tight junctions. The picture that appears here is that of a milieu relatively depopulated of ions, and subject to a very intense transverse electric field. These are two conditions that emerge as necessary in this context. As an interesting corollary, if the fluid being transported would acquire the local concentration in those regions, it would emerge substantially hypotonic. There is some evidence that this may be so, as the coupling coefficient for small currents ($I < 4 \mu\text{A cm}^{-2}$) appears larger than the overall coupling coefficient calculated for the data (*cf.* Fig 3 in Sanchez et al. 2002). Of course, the hypotonic fluid thus generated would tend to be equilibrated via osmotic flows across both apical and basolateral cell membranes.

In conclusion, we propose that for some leaky epithelia, electro-osmotic coupling at the tight junctions could represent one of the basic mechanisms driving fluid transport.

Supported by grant EY06178, NIH (to JF), and in part by Research to Prevent Blindness, Inc. JAH received grants from C.S.I.C. and PEDECIBA (Universidad de la República and Ministerio de Educación y Cultura, Uruguay).

Appendix A

VELOCITY OF WATER FLOW AT THE LEAKY TIGHT JUNCTION

By replacing Eq. 13b, we can obtain the following version of the Brinkman equation Eq. 4:

$$\frac{d^2 v_2}{dx^2} - \frac{v_2(x)}{(L_B)^2} + \frac{1}{\eta} [E_2 F c_{fix}] - \frac{E_2 (\epsilon \epsilon_0)}{\eta (L_{D2})^2} y(x) = 0 \quad (\text{A1a})$$

$$v_2(\delta_2) = 0; v_2(-\delta_2) = 0; (\delta_2 = h_2/2) \quad (\text{A1b})$$

The boundary conditions Eq. A1b imply that there is no water movement at the level of the TJ membranes. The Brinkman's length L_B Eq. A1a depends on viscosity and friction, and is a characteristic of TJ medium. It is given by

$$L_B = \sqrt{\frac{\eta}{k_{fr}}} = \sqrt{K_{per}} \quad (\text{A2})$$

The parameter K_{per} (Eq. A2) has dimensions of area, corresponding to the fractional void volume of the TJ macromolecular media. For known geometries, it can be computed, as in Happel and Brenner (1983). Here, we simply took L_B to correspond to a characteristic length in the TJ, namely, $L_B = h_2 = 45 \text{ \AA}$. As an example, this would result from a TJ in which spheres of 4 \AA in diameter would occupy 0.0065 of the volume, which appears consistent with the geometry depicted schematically in Fig. 2.

The solution of Eqs A1a–A1b is of the form

$$v_2(x) = V_2^{(1)}(x) + V_2^{(2)}(x) \quad (\text{A3a})$$

with

$$V_2^{(1)}(x) = -\frac{1}{\eta} [E_2 F c_{fix}] \frac{[\cosh(x/L_{D2}) - \cosh(\delta_2/L_{D2})]}{L_{D2}^2 \cosh(\delta_2/L_{D2})} \quad (\text{A3b})$$

$$V_2^{(2)}(x) = \frac{\epsilon \epsilon_0 E_2 \beta \zeta_2}{\eta \gamma_2} \coth\left(\frac{\delta_2}{L_{D2}}\right) \left[\frac{\cosh(x/L_B)}{\cosh(\delta_2/L_B)} - \frac{\cosh(x/L_{D2})}{\cosh(\delta_2/L_{D2})} \right] \quad (\text{A3c})$$

We define some auxiliary parameters (γ_1 , γ_2 , α , f , and p):

$$\begin{aligned} \gamma_1 &= \left[1 - \frac{L_B}{L_{D2}} \coth\left(\frac{\delta_2}{L_{D2}}\right) \tanh\left(\frac{\delta_2}{L_B}\right) \right]; \gamma_2 \\ &= \left[1 - \left(\frac{L_{D2}}{\delta_2}\right)^2 \right] \end{aligned} \quad (\text{A4a})$$

$$\begin{aligned} \alpha &= \frac{L_{D2}}{\delta_2} - \frac{1}{\sqrt{\eta} \cosh(F\phi_D/R_g T)}; f \\ &= \left(1 - \frac{L_B}{\delta_2} \tanh\left(\frac{\delta_2}{L_B}\right) \right); p = \alpha \frac{\gamma_1}{\gamma_2} \end{aligned} \quad (\text{A4b})$$

We obtain the water flow in the TJ by integrating Eq. A3a across the TJ width h_2 , and dividing by h_2 . This leads to the result desired, the theoretical water flow though the TJ, already shown in Eq. 14a:

$$\begin{aligned} Q_2(\text{Th}) &= \frac{1}{h_2} \int_{-\delta_2}^{\delta_2} [V_2^{(1)}(x) + V_2^{(2)}(x)] dx \\ &= \frac{F c_{fix} E_2}{\eta} (L_B)^2 f - \frac{\epsilon \epsilon_0 E_2 \zeta_2}{\eta} p \end{aligned} \quad (\text{A4c})$$

Appendix B

ELECTRICAL CONDUCTIVITY OF THE LEAKY TIGHT JUNCTION

As mentioned in the main text, the electrical conductivity of NaCl in free solution, for a concentration $c = 0.15$ mol/L, equals ($\kappa = 21.1 \cdot 10^{-3}$ S/cm. The transference numbers of Na^+ and Cl^- are $t_{\text{Na}} = 0.38$ and $t_{\text{Cl}} = 1 - t_{\text{Na}}$ respectively. The tonic mobilities are related to the electrical conductivity according to

$$\kappa = cF^2(U_{\text{Na}} + U_{\text{Cl}}) \quad (\text{B1})$$

From Eq. B1, we can calculate the corresponding ionic mobilities as $U_{\text{Na}} = (\kappa t_{\text{Na}}/cF^2)$ and $U_{\text{Cl}} = (\kappa t_{\text{Cl}}/cF^2)$. The concentration of each ion in the TJ medium can be determined from Eq. 6. The electrical conductivity of the strand region of the TJ is given by:

$$\kappa_2 = \frac{nb c F^2}{h_2} \left[\int_{-\delta/2}^{\delta/2} \left(U_{\text{Na}} \exp\left(-\frac{F\phi_2(x)}{R_g T}\right) + U_{\text{Cl}} \exp\left(\frac{F\phi_2(x)}{R_g T}\right) \right) dx \right] \quad (\text{B2a})$$

The factor b arises from the volume occupied by the strands protruding into the TJ. If vp is the fractional volume occupied by the strands, it has been shown (Riande, 1972) that:

$$b = \left[\frac{(1 - vp)}{(1 + vp)} \right]^2 \quad (\text{B2b})$$

For our case, we chose $b = 0.45$, corresponding to $vp \approx 0.2$. This appears consistent with current views on the geometry of TJ strand regions (*cf* Fig. 3 in Van Itallie & Anderson, 2004).

The distribution of the electrical potential in the strand region of the TJ (Eq. 13a) can then be used to integrate Eq. B2a:

$$\kappa_2 = \frac{nb c F^2}{h_2} \left[U_{\text{Na}} \exp\left(-\frac{F\phi_D}{R_g T}\right) \int_{-\delta/2}^{\delta/2} \left(1 - \frac{y(x)}{R_g T} \right) dx + U_{\text{Cl}} \exp\left(\frac{F\phi_D}{R_g T}\right) \int_{-\delta/2}^{\delta/2} \left(1 + \frac{y(x)}{R_g T} \right) dx \right] \quad (\text{B3})$$

Substituting for $y(x)$ from (Eq. 13a), Eq B3 can be integrated to yield the expression for the electrical conductivity of the stand region of the TJ shown in

the main text (Eq. 15a).

$$\kappa_2 = F^2 n b c \left[U_{\text{Na}} e^{-F\phi_D/R_g T} \left(1 - \alpha \frac{F\zeta_2}{R_g T} \right) + U_{\text{Cl}} e^{F\phi_D/R_g T} \left(1 + \alpha \frac{F\zeta_2}{R_g T} \right) \right] \quad (\text{B4})$$

Having the conductance κ_2 , the values of interest can now be computed. The specific electrical resistance of the TJ strand region is:

$$R_{\text{str}} = \frac{L_{\text{str}}}{\kappa_2 S_{\text{str}}} \quad (\text{B5})$$

The resistance R_2 of the rest of the TJ is:

$$R_2 = \frac{(L_2 - L_{\text{str}})}{\kappa S_2} \quad (\text{B6})$$

The total resistance of the TJ is:

$$R_{\text{TJ}} = R_{\text{str}} + R_2 \quad (\text{B7})$$

This is the resistance value that is to be compared to those from experiments. The voltage jump ΔV_{str} and the field E_{str} across the strand regions are:

$$\Delta V_{\text{str}} = -R_{\text{str}} \cdot I; \quad E_{\text{str}} = -\frac{\Delta V_{\text{str}}}{L_{\text{str}}} \quad (\text{B8})$$

The field value is used in Eq. 14a to compute water flow.

References

- Barfort, P., Maurice, D.M. 1974. Electrical potential and fluid transport across the corneal endothellium. *Exp. Eye Res.* **19**:11–19
- Bastug, T., Kuyucak, S. 2003. Role of the dielectric constants of membrane proteins and channel water in ion permeation. *Bio-phys. J.* **84**:2871–2882
- Brinkman, H.C. 1947. A calculation of the viscous force exerted by a flowing fluid on a dense swarm of particles. *Appl. Scient. Res.* **A1**:27–35
- Brodoy, D.M. 2002. Motion of nanobeads proximate to plasma membranes during single particle tracking. *Bull. Math. Biol.* **64**:531–563
- Claude, P. 1978. Morphological factors influencing transepithelial permeability: a model for the resistance of the zonula occludens. *J. Membrane Biol.* **39**:219–232
- Claude, P., Goodenough, D.A. 1973. Fracture faces of zonulae occludentes from “tight” and “leaky” epithelia. *J. Cell Biol.* **58**:390–400
- Colegio, O.R., Van Itallie, C., Rahner, C., Anderson, J.M. 2003. Claudin extracellular domains determine paracellular charge selectivity and resistance but not tight junction fibril architecture. *Am. J. Physiol.* **284**:C1346–C1354
- Colegio, O.R., Van Itallie, C.M., McCrea, H J., Rahner, C., Anderson, J.M. 2002. Claudins create charge-selective channels in the paracellular pathway between epithelial cells. *Am. J. Physiol.* **283**:C142–C147
- Donath, E., Pastushenko, V. 1979. Electrophoretical study of cell surface properties. *Bioelectrochem. Bioenerg.* **6**:543–554
- Donath, E., Pastushenko, V., Chizmadjev, Y. 1978. Electroosmotic flow in the hydrodynamic closed chamber. *Studies in Biophysics. J.* **68**:145–154

- Donath, E., Voigt, A. 1986a. Electrophoretic mobility of human erythrocytes. On the applicability of the charged layer model. *Biophys. J.* **49**:493–499
- Donath, E., Voigt, A. 1986b. Streaming current and streaming potential on structured surfaces. *J. Colloid Interface Sci.* **109**:123–139
- Fischbarg, J. 1972. Potential difference and fluid transport across rabbit corneal endothelium. *Biochim. Biophys. Acta* **228**:362–366
- Fischbarg, J., Rubashkin, A., Iserovich, P. 2004. Electro-osmotic coupling in leaky tight junctions is theoretically possible. *In: Experimental Biology 2004*, pp. A710 (Abstract #463.6) FASEB, Washington, D.C.
- Fischbarg, L., Warshavsky, C.R., Lim, J.J. 1977. Pathways for hydraulically and osmotically-induced water flows across epithelia. *Nature* **266**:71–74
- Gross, R.J., Osterle, J.F. 1968. Membrane transport characteristics of ultrafine capillaries. *J. Chem. Phys.* **49**:228–234
- Guo, P., Weinstein, A.M., Weinbaum, S. 2000. A hydrodynamic mechanosensory hypotheses for brush border microvilli. *Am. J. Physiol.* **279**:F698–F712
- Guo, P., Weinstein, A.M., Weinbaum, S. 2003. A dual-pathway ultrastructural model for the tight junction of rat proximal tubule epithelium. *Am. J. Physiol.* **285**:F241–F257
- Hanter, R.J. 1981. Zeta Potential in Colloid Science; Principles and Applications. Academic Press, New York
- Happel, J., Brenner, H. 1983. Low Reynolds Number Hydrodynamics: with Special Applications to Particulate Media. M. Nijhoff; Distributed by Kluwer Boston, The Hague
- Harned, H.S., Owen, B.B. 1958. The Physical Chemistry of Electrolytic Solutions. Reinhold, New York
- Hill, A.E., Shachar-Hill, B., Shachar-Hill, Y. 2004. What are aquaporins for? *J. Membrane Biol.* **197**:1–32
- Hodson, S. 1974. The regulation of corneal hydration by a salt pump requiring the presence of sodium and bicarbonate ions. *J. Physiol.* **236**:271–302
- Jones, I.S. 1979. A theory of electrophoresis of large colloid particles with adsorbed polyelectrolyte. *J. Colloid Interface Sci.* **68**:451–461
- Kaye, G.I., Sibley, R.C., Hoefle, F.B. 1973. Recent studies on the nature and function of the corneal endothelial barrier. *Exp. Eye Res.* **15**:585–613
- Keh, H.J., Liu, Y.C. 1995. Electrokinetic flow in a circular capillary with a surface charge layer. *J. Colloid Interface Sci.* **172**:222–229
- Kruyt, H.R. 1952. Colloid Science. Elsevier, New York
- Kuang K., Ma, L., Sanchez J.M., Fischbarg, J. 2004. Claudin expression and paracellular permeability in cultured rabbit corneal endothelial cells (rec). *Invest. Ophthalmol. Vis. Sci.* **45**:E-Abstract 1090
- Lakshminarayanaiah, N. 1984. Equations of Membrane Biophysics. Academic Press, Orlando
- Larsen, E.H., Sorensen, J.B., Sorensen, J.N. 2002. Analysis of the sodium recirculation theory of solute-coupled water transport in small intestine. *J. Physiol.* **542**:33–50
- Levine, S., Levine, M., Sharp, K.A., Brooks, D.E. 1983. Theory of the electrokinetic behavior of human erythrocytes. *Biophys. J.* **42**:127–135
- Loo, D.D., Wright, E.M., Zeuthen, T. 2002. Water pumps. *J. Physiol.* **542**:53–60
- McLaughlin, S., Mathias, R.T. 1985. Electro-osmosis and the reabsorption of fluid in renal proximal tubules. *J. Gen. Physiol.* **85**:699–728
- Naftalin, R.J., Tripathi, S. 1985. Passive water flows driven across the isolated rabbit ileum by osmotic, hydrostatic and electrical gradients. *360*:27–50
- Pasquale, L.R., Mathias, R.T., Austin, L.R., Brink, P.R., Ciunga, M. 1990. Electrostatic properties of fiber cell membranes from the frog lens. *Biophys. J.* **58**:939–945
- Reuss, L. 2000. General principles of water transport. *In: D.W. Seldin, G. Giebisch*, (editors), *The Kidney, Physiology and Pathophysiology* (chapter 13), pp 321–340, Raven Press, New York
- Reuss, L. 2006 (in press). Mechanisms of water transport across cell membranes and epithelia. *In: R.J. Alpern, S.C. Hebert*, editors. *The Kidney, Physiology and Pathophysiology*. Elsevier, Amsterdam
- Riande, R. 1972. Transfer phenomena in ion-exchange membranes. *In: J. Hladik*, editor. *Physics of Electrolytes*. Academic Press, London, New York
- Romm, E.S., Rubashkin, A.A. 1983. On the thermodynamic theory of the electrokinetic potential on the surface of oxides. *Sov. Elec.* **19**:1348–1352 (English Transl.)
- Rubashkin, A.A. 1989. Structure of the electric double layer at the interface between a microporous ion-exchange membrane and an electrolyte solution. *Sov. Elec.* **25**:571–578 (English Transl.)
- Sanchez, J.M., Li, Y., Rubashkin, A., Iserovich, P., Wen, Q., Ruberti, J.W., Smith, R.W., Rittenband, D., Kuang, K., Diecke, F.P.J., Fischbarg, J. 2002. Evidence for a Central Role for Electro-Osmosis in Fluid Transport by Corneal Endothelium. *J. Membrane Biol.* **187**:37–50
- Sasidhar, V., Ruckenstein, E. 1981. Electrolyte osmosis through capillaries. *J. Colloid Interface Science* **82**:439–456
- Schmid, G. 1950. Zur Elektrochemie feinporiger Kapillarsysteme. *Z. Electrochem.* **54**:424–430
- Schmid, G., Schwarz, H. 1952. Zur Elektrochemie feinporiger Kapillarsysteme. V. Stromungspotentiale: Donnan-Behinderung des Elektrolytdurchgangs bei Strömungen. *Z. Elektrochem.* **56**:35–44
- Shachar-Hill, B., Hill, A.E. 2002. Paracellular fluid transport by epithelia. *Int. Rev. Cytol.* **215**:319–350
- Starov, V.M., Bowen, W.R., Welfoot, J.S. 2001. Flow of multi-component electrolyte solution through narrow pores of nanofiltration membranes. *J. Colloid Interface Science* **240**:509–524
- Starov, V.M., Solomentsev, Y.E. 1993. Influence of gel layer on electrokinetic phenomena. 1. Streaming potential. *J. Colloid Interface Science* **158**:159–165
- Tada, S., Tarbell, J.M. 2000. Interstitial flow through the internal elastic lamina affects shear stress on arterial smooth muscle cells. *Am. J. Physiol.* **278**:H1589–H1597
- Tikhomolova, K.P., Kemp, T.J. 1993. Electro-osmosis. E. Horwood, New York
- Van Itallie, C.M., Anderson, J.M. 2004. The molecular physiology of tight junction pores. *Physiology* **19**:331–338
- Vorotyntsev, M.A., Ermakov, Y.A., Markin, V.S., Rubashkin, A.A. 1993. Distribution of the interfacial potential drop in a situation when ionic solution components enter a layer of finite thickness with fixed space charge. *Russian J. Electrochem.* **29**:513–523
- Vorotyntsev, M.A., Rubashkin, A.A., Badiali, J.P. 1996. Potential distribution across the electroactive-polymer film between the metal and solution as a function of the film charging level. *Electrochimica Acta* **41**:2313–2330
- Weinstein, A.M. 2003. Mathematical models of renal fluid and electrolyte transport: acknowledging our uncertainty. *Am. J. Physiol.* **284**:F871–F884
- Weinstein, A.M., Windhager, E.E. 2001. The paracellular shunt of proximal tubule. *J. Membrane Biol.* **184**:241–245
- Wunderlich, R.W. 1982. The effects of surface structure on the electrophoretic mobilities of large particles. *J. Colloid. Interface Sci.* **88**:385–397
- Zeuthen, T. 2002. General models for water transport across leaky epithelia. *Int. Rev. Cytol.* **215**:283–317